Diffuse Scattering Measurements of Static Atomic Displacements in Crystalline Binary Solid Solutions

G.E. Ice, C.J. Sparks, X. Jiang, and L. Robertson
Oak Ridge National Laboratory, Oak Ridge, TN 37831-6118

(Submitted 27 January 1998; in revised form 15 July 1998)

Diffuse x-ray scattering from crystalline solid solutions is sensitive to both local chemical order and local bond distances. In short-range ordered alloys, fluctuations of chemistry and bond distances break the long-range symmetry of the crystal within a local region and contribute to the total energy of the alloy. Recent use of tunable synchrotron radiation to change the x-ray scattering contrast between elements has greatly advanced the measurement of bond distances between the three kinds of atom pairs found in crystalline binary alloys. The estimated standard deviation on these recovered static displacements approaches ±0.001 Å (±0.0001 nm), which is an order of magnitude more precise than obtained with extended x-ray absorption fine structure measurement. In addition, both the radial and tangential displacements can be recovered to five near neighbors and beyond. These static displacement measurements provide new information that challenges the most advanced theoretical models of binary crystalline alloys.

1. Introduction

Although atomic size differences have long been recognized as critical to alloy design, experimental measurements of atomic size in crystalline alloys have been indirect or marginally precise. The recent availability of tunable x-rays from synchrotron sources now allows diffuse scattering measurements where the x-ray scattering contrast between the different elements in the sample can be enhanced or reduced. This has led to meaningful recovery of individual pair displacements to typically ±0.001 Å (±0.0001 nm) (Ref 1-4). In a binary alloy of *A* and *B* atoms, the *AA*, *AB*, and *BB* average pair separation can be determined out to five or more atom shells (near neighbors). This new information presents a challenge to the theoretical community; theoretical models must allow for relaxation of the atoms away from the sites of the average lattice.

The long-range effect of substitutional alloying on the alloy lattice parameter is well characterized. The addition of large *A* atoms to an alloy with small *B* atoms expands the lattice constant from the pure *B* value. This is observed to be the case with a nearly linear response of the lattice constant to concentration throughout the solubility range and is often referred to as Vegard's law (Ref 5). Many models have been proposed to explain this linear relationship between the lattice parameter and elemental concentration (Ref 5-7). Though these models reproduce the nearly linear change in lattice parameter with concentration, actual measurements of the individual pair distances to test both models and theories have been almost nonexistent or of questionable accuracy.

The local effect of atomic size plays an important, but still poorly understood, role in alloy behavior. That atomic size disparity between solvent and solute affects solubility and the physical/chemical properties of alloys is well known. In a discussion of atomic size in alloys, Laves (Ref 8) shows that the ratio of the atomic radii of the components affects their crystal symmetry. Solid solution strengthening or hardening increases with atomic size difference (Ref 9). Though Hume-Rothery (Ref 10) recognized the role of atomic size differences on the structure and phase stability of alloys, the role and definition of atom size in metals with free electrons has remained elusive. Recent theoretical considerations stress the need to include static displacements in calculations of total energy (Ref 11).

The most often quoted chemical displacements from an average lattice are obtained from extended x-ray absorption fine structure (EXAFS) measurements. EXAFS measurements are usually made in dilute alloys with the assumption that all nearest-neighbor (nn) pairs to a solute atom are solvent atoms (Ref 12, 13). EXAFS precision is typically 0.02 Å (0.002 nm), and at best 0.01 Å (0.001 nm), which for most alloys is marginal for measurement of the deviations of the atom pair spacings from the average long-range spacing. See Ref 12 and 13 and references contained therein for a general discussion of EXAFS measurements and results.

Though diffuse scattering with x-rays (neutrons and electrons) has been used since 1951 to provide information on the displacement of the atoms from the sites of the average lattice (Ref 14, 15), the practice of separating the individual pair displacements with selected x-ray energies has only been developed recently (Ref 1-4). Details of the x-ray measurements and data analysis to recover bond distances in alloys are found in Ref 4 and 16. Here the focus is on the reliability and implication of the average bond distances recovered from crystalline binary alloys with the so-called "three x-ray energy" or "3λ" technique.

The information recovered is presented with an emphasis on the static displacements of the atoms from the sites of the average lattice. Sufficient description is given so that the physical meaning of the displacements recovered from diffuse scattering data can be understood by the nonspecialist. The discussion is confined to x-ray diffuse scattering measurements

made on crystalline binary solid solution alloys where the average lattice is well defined by sharp (unbroadened) Bragg reflections. Defects such as stacking faults, high dislocation densities as from cold working, displacive transformation, incoherent precipitates, and other defects that can broaden, split, or produce new Bragg reflections are precluded as leaving an ill-defined average lattice. Such defects are treated elsewhere (Ref 17).

For crystalline solid solutions, the regular d spacing between crystallographic planes is maintained for hundreds, even thousands of planes as shown in Fig. 1; atoms are displaced out of these average planes in such a way as to maintain a regular d spacing. In order to define the static displacements to ±0.001 Å (±0.0001 nm) from this average lattice, the average planar spacing should vary by less than ±0.001 Å (±0.0001 nm). On differentiating Bragg's law, we obtain:

$$\frac{\Delta d}{d} = \Delta\theta \cot\theta \qquad \text{(Eq 1)}$$

Here, θ is the half angle between the incident and scattered x-ray. For a scattering angle of $2\theta = 40°$, an average d spacing of 2 Å, and an error in Δd of ±0.001 Å (±0.0001 nm), then $\Delta\theta = 0.01°$ and the Bragg reflection would be broadened by $\Delta 2\theta = 0.02°$. Substitutional crystalline solid solutions typically have sharper Bragg reflections than this 0.02° full width-half maximum (FWHM).

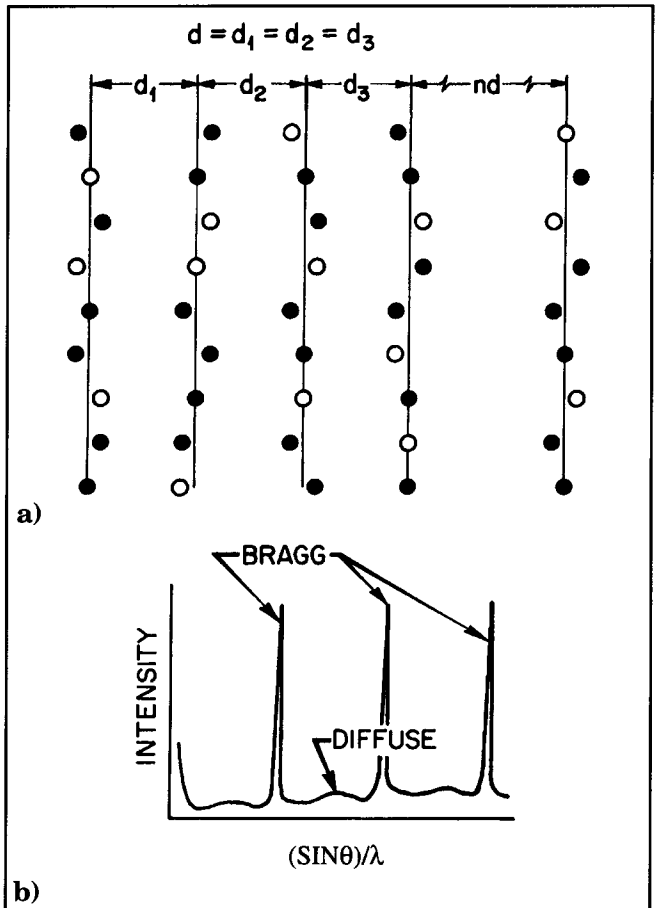

Fig. 1 (**a**) Displacement about the average lattice preserves the regular spacing between atomic planes such that $d = d_1 = d_2 = d_3$, ... The average lattice is obtained from (**b**) the positions of the sharp Bragg reflections. Information about short-range correlations among the atoms is contained in the diffusely distributed intensity between the Bragg peaks.

2. Pair Correlations from Diffuse Scattering: Diffraction Theory of Static Displacement Terms

This section begins with a brief overview of the kinematic diffraction theory in which the weak diffuse scattering can be approximated without extinction effects (first Born approximation). The purpose of this overview is to define the pair correlation parameters recovered from diffuse scattering measurements. Definitions of the atomic displacements are illustrated in Fig. 2.

The elastically scattered x-ray (neutron) intensity in electron units (eu) per atom from an ensemble of atoms is given by:

$$I(\mathbf{h}) = \sum_p \sum_q f_p f_q \, e^{2\pi i \mathbf{h}\cdot(\mathbf{r}_p - \mathbf{r}_q)} \qquad \text{(Eq 2)}$$

where f_p and f_q denote the complex x-ray atomic scattering factor (or neutron scattering lengths), p and q designate the lattice sites, $\mathbf{r}_p$ and $\mathbf{r}_q$ are the position vectors for those sites, and $\mathbf{h}$ is the momentum transfer or reciprocal lattice vector $|\mathbf{h}| = (2 \sin\theta)/\lambda$. For crystalline solid solutions in which the Bragg reflections are sharp and the average lattice is well-defined, the atom

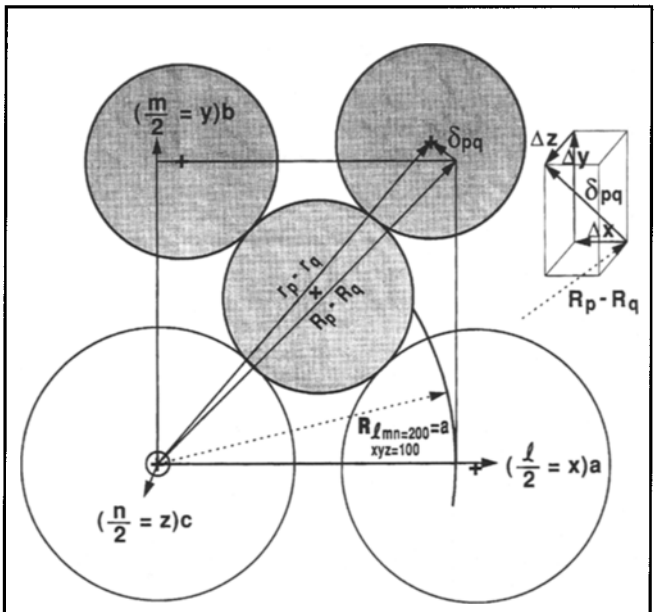

Fig. 2 Schematic of a crystalline solid solution with atom pairs displaced by δ_{pq} from the average lattice vector $\mathbf{R}_p - \mathbf{R}_q$. The + symbols represent the atom centers. The displacements are given in terms of their *lmn* components designated $\Delta\mathbf{X}_{lmn}$, $\Delta\mathbf{Y}_{lmn}$, $\Delta\mathbf{Z}_{lmn}$ where $l = 2x$, $m = 2y$, and $n = 2z$ from an earlier convention for the designation of atom shells as integers.

positions can be represented by $\mathbf{r} = \mathbf{R} + \bar{\delta}$ where $\mathbf{R}$ is determined from the lattice constant and $\bar{\delta}$ is the displacement of the atom from that average lattice. The exponential term is written:

$$e^{2\pi i\,\mathbf{h}\cdot[(\mathbf{R}_p-\mathbf{R}_q)+(\bar{\delta}_p-\bar{\delta}_q)]} \equiv e^{2\pi i\,\mathbf{h}\cdot(\mathbf{R}_p-\mathbf{R}_q)}\, e^{2\pi i\,\mathbf{h}\cdot(\bar{\delta}_p-\bar{\delta}_q)} \quad \text{(Eq 3a)}$$

and

$$e^{2\pi i\,\mathbf{h}\cdot(\bar{\delta}_p-\bar{\delta}_q)} \equiv e^{ix} = 1 + ix - \frac{x^2}{2!} - i\frac{x^3}{3!} + \ldots + i^j\frac{x^j}{j!} + \ldots \quad \text{(Eq 3b)}$$

where j is an integer.

This series expansion converges rapidly when $\mathbf{h}\cdot\bar{\delta}$ is sufficiently small. Upon substitution of Eq 3(b) into Eq 2, the total intensity for a crystalline binary alloy can be written as:

$$I_T = I_{FUND} + I_{SRO} + I_{1SD} + I_{j\geq 2} \quad \text{(Eq 4)}$$

$I_{FUND} + I_{SRO}$ represents the first term of the series expansion, I_{1SD} represents the second term (ix) of Eq 3(b), and $I_{j\geq 2}$ represents the remainder. Following the treatment of Warren and coworkers (Ref 17), the terms for a cubic crystalline substitutional binary alloy are written as:

$$I_{FUND} = |c_A f_A + c_B f_B|^2 \sum_p \sum_q e^{2\pi i\,\mathbf{h}\cdot(\mathbf{R}_p-\mathbf{R}_q)} \quad \text{(Eq 5)}$$

$$\frac{I_{SRO}}{N} = c_A c_B |f_A - f_B|^2 \sum_{lmn} \alpha_{lmn}\, e^{-2M\Phi_{lmn}} \cos\left[\pi(h_1 l + h_2 m + h_3 n)\right] \quad \text{(Eq 6)}$$

$$\frac{I_{1SD}}{N} = -\frac{2\pi}{a} c_A c_B \sum_{lmn} \sin\left[\pi(h_1 l + h_2 m + h_3 n)\right] \left\{\left[\frac{c_A}{c_B} + \alpha_{lmn}\right] \times \mathrm{Re}\left[f_A(f_A - f_B)^*\right]\left[h_1\langle\Delta\mathbf{X}^{AA}_{lmn}\rangle + h_2\langle\Delta\mathbf{Y}^{AA}_{lmn}\rangle + h_3\langle\Delta\mathbf{Z}^{AA}_{lmn}\rangle\right] - \left[\frac{c_B}{c_A} + \alpha_{lmn}\right] \mathrm{Re}\left[f_B(f_A - f_B)^*\right]\left[h_1\langle\Delta\mathbf{X}^{BB}_{lmn}\rangle + h_2\langle\Delta\mathbf{Y}^{BB}_{lmn}\rangle + h_3\langle\Delta\mathbf{Z}^{BB}_{lmn}\rangle\right]\right\} \quad \text{(Eq 7)}$$

Here c_A is the A atom fraction of N atoms of a binary alloy, c_B is the B atom fraction, f_A and f_B are the respective complex atomic scattering factors, and Re denotes the real part of a complex number. The lattice parameter of the cubic system is a; lmn are the coordinates of the atom positions relative to the origin of the average lattice as shown in Fig. 2; and h_1, h_2, and h_3 are the Cartesian coordinates of the momentum transfer vector $\mathbf{h}$ in reciprocal lattice units (rlu). The Warren-Cowley short-range order coefficient $\alpha_{lmn} = 1 - p^{AB}_{lmn}/c_B$, where p^{AB}_{lmn} is the conditional probability that after finding an A atom at lmn there is a B atom at the origin (Ref 17). The displacements $\bar{\delta}_p - \bar{\delta}_q \equiv \bar{\delta}_{lmn} \equiv \Delta\mathbf{X}_{lmn} + \Delta\mathbf{Y}_{lmn} + \Delta\mathbf{Z}_{lmn}$ are illustrated in Fig. 2.

The average over all possible pairs that can be formed of the $\mathbf{X}$ components of the pair displacements for AA pairs with relative coordinates lmn are given by $\langle\Delta\mathbf{X}^{AA}_{lmn}\rangle$ and similarly for $\mathbf{Y}$ and $\mathbf{Z}$ in the same units as the lattice constant. The average displacements for AB pairs $\langle\Delta\mathbf{X}^{AB}_{lmn}\rangle$ or their $\mathbf{Y}$ and $\mathbf{Z}$ components can be derived from the AA and BB displacements. By definition, the displacements are deviations from the average lattice; the weighted average of the displacements $\langle\bar{\delta}_{lmn}\rangle$ for all AA, AB, BA, and BB pairs for any coordination shell is zero. Hence:

$$c_A p^{AA}_{lmn}\langle\bar{\delta}^{AA}_{lmn}\rangle + c_A p^{BA}_{lmn}\langle\bar{\delta}^{BA}_{lmn}\rangle + c_B p^{AB}_{lmn}\langle\bar{\delta}^{AB}_{lmn}\rangle + c_B p^{BB}_{lmn}\langle\bar{\delta}^{BB}_{lmn}\rangle = 0 \quad \text{(Eq 8a)}$$

When rewritten in terms of αs with $c_A p^{BA} = c_B p^{AB}$, and with $\langle\bar{\delta}^{AB}_{lmn}\rangle = \langle\bar{\delta}^{BA}_{lmn}\rangle$, it is determined that:

$$2(\alpha_{lmn} - 1)\langle\Delta\mathbf{X}^{AB}_{lmn}\rangle = \left[\frac{c_A}{c_B} + \alpha_{lmn}\right]\langle\Delta\mathbf{X}^{AA}_{lmn}\rangle + \left[\frac{c_B}{c_A} + \alpha_{lmn}\right]\langle\Delta\mathbf{X}^{BB}_{lmn}\rangle \quad \text{(Eq 8b)}$$

Equation 8(b) ensures that the interatomic vector averaged over all pairs in the crystal for each lmn coordination shell is consistent with the average lattice long-range lattice parameter (Ref 14). For example $\mathbf{r}_{200}$ summed for all AA, AB, and BB $\langle 200\rangle$ pairs and divided by the number of pairs must equal the crystal lattice constant (the average unit cell size, a). No assumption is made as to how the displacements are distributed about the average. This information is contained in the higher moments. Thus there are only two independent pair displacements for each shell of a cubic crystalline binary alloy. Equation 7 can be written in terms of any two of the three individual pair displacements according to Eq 8(b). For widely separated atoms, the first moment of the displacements goes to zero because they are equally likely to be displaced in a positive or negative direction relative to the atom at the origin. To evaluate the contribution from the term $I_{j\geq 2}$, it is assumed that either the quadratic and high-order terms in this series expansion of the thermal and static displacements are the same for AA, AB, and BB atom pairs or that the different elements have nearly the same x-ray atomic scattering factors (Ref 1-4). This approximation is good for alloys with elements nearby in the periodic table, as is the case of Fe-Ni, Cr-Fe, and Cr-Ni alloys that have been studied to date. These alloys have similar masses (similar thermal motions), similar sizes (small static displacements), and similar numbers of electrons (similar x-ray scattering factors). With this approximation, these remaining terms of the series expansion can be written as:

$$\frac{I_{j\geq 2}}{N} = |c_A f_A + c_B f_B|^2 \frac{i^j}{j!} \sum_{lmn} \langle(\mathbf{h}\cdot\bar{\delta}_{lmn})^j\rangle\, e^{2\pi i\,\mathbf{h}\cdot\mathbf{R}_{lmn}} + c_A c_B |f_A - f_B|^2 \frac{i^j}{j!} \sum_{lmn} \alpha_{(lmn)}\langle(\mathbf{h}\cdot\bar{\delta}_{lmn})^j\rangle\, e^{2\pi i\,\mathbf{h}\cdot\mathbf{R}_{lmn}} \quad \text{(Eq 9)}$$

The first term of Eq 9 weakens the fundamental Bragg reflections and distributes this intensity as temperature and static diffuse scattering. The second term of Eq 9 weakens the superlattice reflections associated with long-range order or, as is the case here, weakens the short-range order (SRO) diffuse maxima when there is only local order.

The second term of Eq 9, which contains α_{lmn}, has been treated by Walker and Keating (Ref 18) and is included as a thermal like factor $e^{-M\varphi_{lmn}}$ in Eq 6. The effect of including this term on recovered αs is not more than 2% at room temperature (Ref 2, 4). The first term of Eq 9 includes quadratic and higher-order thermal scattering and a smaller static diffuse scattering contribution. Typically, the quadratic static scattering is less than the quadratic thermal scattering by a factor of three or more at room temperature, even for alloys with large atomic size differences (e.g., $AuCu_3$) (Ref 19). Because the first term of Eq 9 depends on $(c_A f_A + c_B f_B)^2$, its separation from I_{SRO} and I_{1SD} (which depend on $f_A - f_B$) can be accomplished by choosing an x-ray energy such that $f_A - f_B \approx 0$. Thus, the first term of Eq 9 can be measured separately from $I_{SRO} + I_{1SD}$ at one energy and scaled by $(c_A f_A + c_B f_B)^2$ to other energies. Measurements at three different x-ray energies and the recovery of the αs and δs are described in Ref 1 to 4. A nonlinear least-square fit to all three data sets is refined simultaneously with a program that includes the statistical errors on the input data (Ref 4).

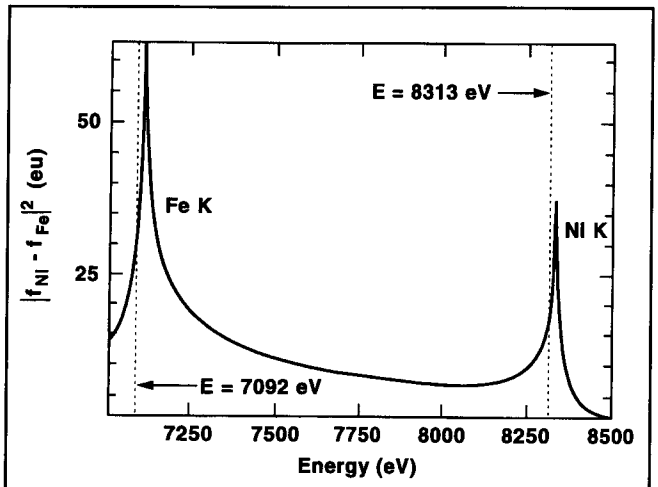

Fig. 3 The variation in the Laue scattering term $|f_{Ni} - f_{Fe}|^2$ with x-ray energy in the vicinity of the Fe and Ni K absorption edges permits selection of x-ray energies to change the contrast for recovery of the local chemical order and displacements among the individual atom pairs.

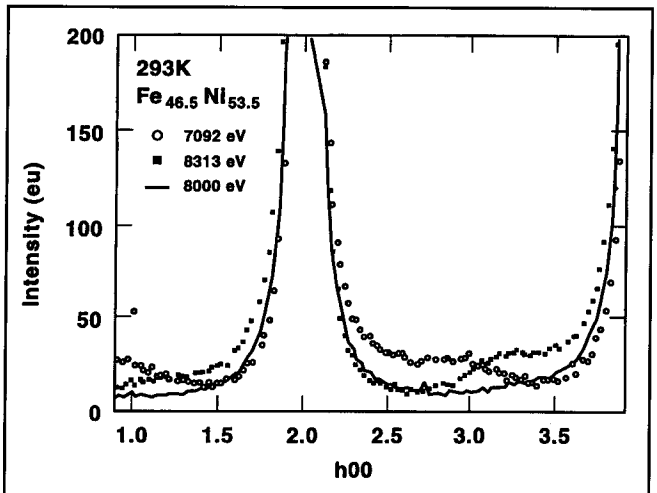

Fig. 4 Total elastically scattered x-ray intensity along the ⟨h00⟩ measured at 293 K for the three x-ray energies listed. Note the shift in contrast for intensities measured with energies 20 eV below the Fe K edge at 7092 eV and the Ni K edge at 8313 eV, which changes the sign of Re $(f_{Ni} - f_{Fe})$. The outlying data point at the {100} position is from harmonic energy contamination of the incident radiation and such points are removed before processing.

The precision with which the displacements can be recovered depends in part on how significant the term Eq 7 is relative to the term Eq 6, and on how large a contrast change can be effected in f_A $(f_A - f_B)^*$; with x-rays the scattering contrast varies with energy near the atomic absorption edges (Ref 4). For atoms nearby in the periodic table, the contrast can actually be reversed, and because $|f_A - f_B|$ is small, the displacement term containing f_A $(f_A - f_B)$ is large compared to the short-range order term containing $(f_A - f_B)^2$.

For Fe and Ni alloys, $(f_A - f_B)^2$ can be made to approach zero by proper choice of x-ray energy (near 8500 eV) as shown in Fig. 3. The quadratic, higher-order thermal and static displacement scattering, along with the smearing functions of the experimental arrangement and possible multiple-scattering processes, are approximately removed by subtracting the scaled null Laue data. Though the assumption is made here that the *A* and *B* atoms have similar quadratic and higher-order displacements, possible errors introduced by this assumption are minimized by the choice of alloys with atoms of similar masses. The previous practice of calculating the thermal diffuse scattering (TDS) from force constants also assumes that constituent atoms have the same quadratic and higher-order displacements. However, the use of force constants makes the harmonic approximation and ignores both the high-frequency acoustical and optical modes and the short-range correlations important to the scattering at the zone boundaries. All this is included in the measured null Laue scattering.

An example of the raw data measured for three different x-ray energies from an $Fe_{46.5}Ni_{53.5}$ alloy is shown in Fig. 4 (Ref 4). The solid line in Fig. 4 is the near-null Laue measurement of the quadratic and higher-order displacement terms, which is removed form the other data sets to recover the αs and the δs. Comparison of x-ray results with neutron diffuse scattering measurements that energy-discriminate against thermal contributions gives very similar αs for Fe_3Ni (Ref 4).

3. Statistical and Systematic Errors

The statistical uncertainties of the recovered parameters are estimated by propagating the standard deviation, $\pm\sqrt{n}$, of the total number of counts, *n*, for each data point through the nonlinear least-squares processing of the data. Systematic errors were determined by changing the values of input variables, such as the x-ray atomic scattering factors, and reprocessing the data.

As input parameters were varied, the intensities were rescaled so that the I_{SRO} values are positive everywhere and match values at the origin of reciprocal space measured by small-angle scattering. The integrated Laue scattering over a repeat volume in reciprocal space is also constrained to have an average value of $c_A\, c_B\, (f_A - f_B)^2$; $\alpha_{000} = 1$. These two constraints eliminate most of the systematic errors associated with converting the raw intensities into absolute units (Ref 20). The intensities measured at two different energies are adjusted to within ~1% on a relative scale, and the intensity at the origin is matched to measured values. For these reasons, the standard deviations for α_{000} are estimated at ~1%.

Errors on the recovered αs and ΔXs arising from statistical and various possible systematic errors in the measurement and analysis of diffuse scattering data are given in Tables 1 and 2 for the $Fe_{46.5}Ni_{53.5}$ alloy (Ref 4, 20-22). Details of parameters used in the conversion to absolute intensity units are given in Ref 2 and 17. A previous assessment of the systematic errors without the constraint of forcing $\alpha = 1$, and without keeping the intensity at the origin and fundamentals a positive match to known values, resulted in estimated errors being 2 to 5 times larger than those reported here (Ref 21). Parameters necessary to the analysis of the data (other than well-known physical constants) with the best estimate of their standard deviations and their contributing standard deviations to the αs and ΔXs are listed in Tables 1 and 2. From a comparison of theoretical and measured values, the following errors are estimated: a 0.2 eu error on the real part of the x-ray atomic scattering factors, a

Table 1 Standard Deviation of ±1σ for the Uncertainties in the Warren-Cowley Short-Range Order Parameter, α, of $Fe_{46.5}Ni_{53.5}$ for Statistical and Possible Systematic Errors

lmn	α_{lmn} (σ_{Total})	$\sigma(\sqrt{n})$	$\sigma(f')$, ±0.2 eu	$\sigma(p_0)$, ±1%	σ(RRS), ±1 eu	$\sigma_{Compton}$	$\sigma(c_A)$, ±0.3 at.%
000	1.0000 (100)	0.0024	0	0	0	0	0
110	–0.0766 (54)	0.0018	0.0010	0.0048	0	0.0006	0.0011
200	0.0646 (28)	0.0017	0.0003	0.0016	0.0008	0.0013	0.0003
211	–0.0022 (15)	0.0014	0	0.0004	0.0001	0.0002	0.0001
220	0.0037 (14)	0.0013	0.0002	0.0003	0.0003	0.0003	0.0001
310	–0.0100 (11)	0.0011	0.0001	0.0002	0.0001	0.0001	0.0001
222	0.0037 (12)	0.0011	0	0.0002	0.0002	0.0003	0
321	–0.0032 (19)	0.0009	0	0.0001	0.0001	0.0001	0.0001
400	0.0071 (12)	0.0011	0.0002	0.0001	0.0003	0.0004	0
330	–0.0021 (9)	0.0008	0.0001	0	0.0003	0.0001	0
411	0.0007 (7)	0.0007	0	0	0	0.0002	0
420	0.0012 (8)	0.0007	0.0002	0	0.0004	0.0001	0
332	–0.0007 (7)	0.0007	0	0	0	0.0001	0

Total error is shown in parentheses; 0 indicates uncertainties less than 0.00005.

Table 2 Standard Deviation of ±1σ of *x*, *y*, and *z* Components of the Pair Fe-Fe Displacements $\bar{\delta}_{Fe\text{-}Fe}$ for the Various Atom Pairs of $Fe_{46.5}Ni_{53.5}$ for Statistical and Possible Systematic Errors

lmn	ΔX(σ_{Total}), Å	$\sigma(\sqrt{n})$	$\sigma(f')$, ±0.2 eu	$\sigma(p_0)$, ±1%	σ(RRS), ±1 eu	$\sigma_{Compton}$	$\sigma(c_A)$, ±0.3 at.%
110	0.0211 (25)	0.0002	0.0023	0.0007	0.0002	0.0004	0.0004
200	–0.0228 (14)	0.0004	0.0010	0.0007	0.0002	0.0004	0.0002
211	0.0005 (2)	0.0002	0	0.0001	0.0001	0	0
121	0.0014 (4)	0.0001	0.0003	0.0001	0.0002	0	0
220	0.0030 (7)	0.0002	0.0006	0.0001	0.0003	0.0001	0
310	0.0022 (3)	0.0002	0.0001	0.0001	0.0002	0.0001	0
130	0.0009 (2)	0.0002	0.0001	0	0.0001	0	0
222	0.0003 (3)	0.0002	0.0002	0	0.0001	0	0
321	0.0011 (2)	0.0001	0.0001	0	0.0002	0	0
231	0.0001 (1)	0.0001	0	0	0.0001	0	0
123	0.0008 (4)	0.0001	0.0001	0	0	0	0
400	–0.0019 (6)	0.0004	0.0002	0.0001	0.0003	0.0001	0
330	0.0011 (4)	0.0002	0.0001	0	0.0003	0	0
411	–0.0008 (3)	0.0002	0.0002	0	0.0002	0	0
141	–0.0001 (2)	0.0001	0.0001	0	0.0001	0	0

Total error is shown in parentheses; 0 indicates uncertainties less than 0.00005 Å.

1% error in the P_0 calibration for converting the raw intensities to absolute units (eu), a 1 eu error in separating the inelastic resonant-Raman scattering (Ref 23), a 0 to 1 eu **h** dependent Compton scattering error, and an error of ±0.3 at.% in composition (Ref 4, 22). Systematic errors are larger than the statistical errors for the first three shells.

The asymmetric contribution of the first moment of the static displacements, I_{1SD} (Eq 7), to the diffuse intensity I_{SRO} + I_{1SD} for an $Fe_{63.2}Ni_{36.8}$ alloy is displayed in Fig. 5 (Ref 24). Without static displacements, the I_{SRO} maxima would occur at the 100 and 300 superlattice positions. The static atomic displacements for the alloy are similar to those given in Table 2. Such large distortions of the short-range order diffuse scattering caused by displacements of <0.02 Å (<0.002 nm) emphasize the sensitivity of this technique. When x-ray energy is changed from 7.092 to 8.313 keV, f_{Ni} becomes smaller than f_{Fe}. Figure 5 displays a reversal in the shift of the position of the diffuse scattering maxima. These two x-ray energies were chosen for the 3λ method to emphasize this contrast, and a third was chosen nearest the null Laue energy for removal of the TDS. The total estimated standard deviation on the values of the αs, and in particular the **ΔX**s, give unprecedented precision for the displacements with errors ±0.003 Å (±0.0003 nm) and less.

4. Static Atomic Displacements

4.1 Meaning of Recovered Static Displacements

Because the x-ray beam is about a millimeter in diameter and penetrates a few microns into the sample, ~10^{17} atoms contribute to the diffraction pattern with ~10^{18} first neighbor pairs. From Eq 3(a):

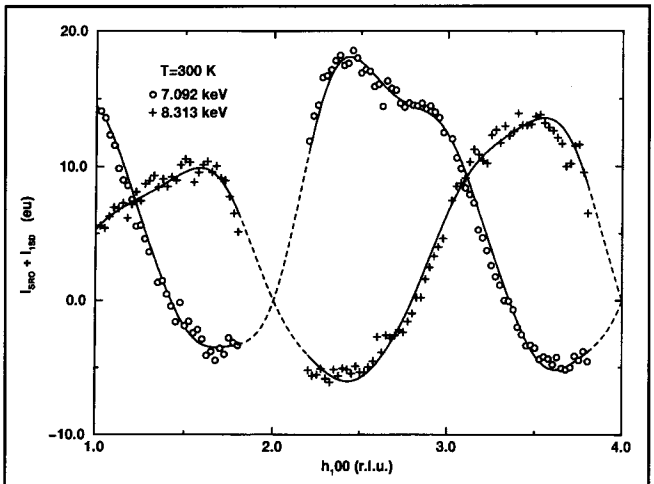

Fig. 5 Diffusely scattered x-ray intensity from an $Fe_{63.2}Ni_{36.8}$ Invar alloy associated with the chemical order I_{SRO} and the first moment of the static displacements I_{1SD} along the [$\mathbf{h}_1$00] direction. A major intensity change is affected by the choice of two different x-ray energies. The solid lines calculated from the αs and δs recovered from the 3λ data sets closely fit the observed data given by Υ and +. The dashed lines are calculated intensity through the fundamental reflections. Source: Ref 24.

$$\mathbf{r}_p - \mathbf{r}_q = (\mathbf{R}_p - \mathbf{R}_q) + (\bar{\delta}_p - \bar{\delta}_q) \quad \text{(Eq 10)}$$

and the frame of reference can be moved so that its origin always resides on one of the atoms of the pair, such that $\mathbf{r}_p \equiv \mathbf{r}_0 \equiv 0$, $\mathbf{R}_p \equiv \mathbf{R}_0 \equiv 0$, and $\delta_p \equiv \delta_0 \equiv 0$, then:

$$\mathbf{r}_p - \mathbf{r}_q = \mathbf{r}_0 - \mathbf{r}_q = \mathbf{r}_0 - \mathbf{r}_{lmn} = -\mathbf{r}_{lmn} \quad \text{(Eq 11)}$$

and with the atom pair identified by *ij*:

$$\mathbf{r}^{ij}_{lmn} = \mathbf{R}_{lmn} + \bar{\delta}^{ij}_{lmn} \quad \text{(Eq 12)}$$

where $\mathbf{R}_{lmn}$ is independent of the kinds of atom pairs because it is defined by the average lattice, that is, Bragg reflection positions. The average value of the measured $\mathbf{r}_{lmn}$ for all the *N* pairs contributing to the measured intensity is:

$$\langle \mathbf{r}^{ij}_{lmn} \rangle = \frac{1}{N^{ij}} \sum_{ij} \langle \mathbf{R}_{lmn} + \bar{\delta}^{ij}_{lmn} \rangle = \mathbf{R}_{lmn} + \langle \bar{\delta}^{ij}_{lmn} \rangle \quad \text{(Eq 13)}$$

Here $\langle \bar{\delta}^{ij}_{lmn} \rangle$ is the variable recovered from the diffuse scattering. As shown in Eq 7, the rectangular coordinates of the average displacement vector can be recovered:

$$\langle \bar{\delta}^{ij}_{lmn} \rangle \equiv \langle \Delta \mathbf{X}^{ij}_{lmn} \rangle + \langle \Delta \mathbf{Y}^{ij}_{lmn} \rangle + \langle \Delta \mathbf{Z}^{ij}_{lmn} \rangle \quad \text{(Eq 14)}$$

For cubic systems when the atom has less than 24 neighboring atoms in a coordination shell (permutations and combinations of ±*l*, ±*m*, ±*n*), $\langle \bar{\delta}^{ij}_{lmn} \rangle$ must be parallel to the interatomic vector $\mathbf{R}_{lmn}$. This maintains the statistically observed long-range cubic symmetry even though on a local scale this symmetry is broken. For *lmn* multiplicities ≥24, the displacements, on the average, need not be parallel to the average interatomic vector $\mathbf{R}_{lmn}$ to preserve cubic symmetry (Ref 25).

Measurements of diffuse scattering from single crystals provides the vector components of the atomic displacements ⟨**ΔX**⟩, ⟨**ΔY**⟩, and ⟨**ΔZ**⟩; whereas the spherical average obtained from EXAFS and x-ray measurements on amorphous materials and crystalline powders gives only the magnitude of the radial displacements. Thus, diffuse x-ray scattering provides new information about the vector displacements associated with near-neighbor chemistry.

4.2 Discussion of Measured Displacements

Measured displacements such as those presented in Table 2 provide unique insight into how atoms move off their lattice sites when local symmetry is broken. Local symmetry is broken when a multicomponent crystalline material is above the ordering temperature (with less-than-perfect long-range order) and/or off-stoichiometry. With perfect long-range order, the atoms are constrained to lie precisely on the sites of the average lattice by balanced forces. In alloys where the local symmetry is broken, new insights are gained into the chemically distinct bonding, including the interatomic bond distances and whether the displacements have both radial and tangential

components. With reference to Fig. 2, the displacement for the [110] nearest-neighbor atoms is, on average, radial with a magnitude given by $|\langle\bar{\delta}_{110}\rangle| = \sqrt{2}|\Delta\mathbf{X}_{110}|$.

Note that the Fe-Fe first-neighbor pair distances given in Table 2 are 0.021(3) Å · $\sqrt{2}$ = 0.030(4) Å further apart than the average lattice and that second neighbor pairs are closer by (–) 0.023(1) Å. Average bond distances along the interatomic vector between nearest-neighbor pairs for this fcc lattice are obtained by adding the $\sqrt{2}|\Delta\mathbf{X}_{110}|$ to the average interatomic vector $\mathbf{R}_{110}$ as defined in Fig. 2. $|\mathbf{R}_{110}|$ is just the cubic lattice constant, a, times $1/\sqrt{2}$. From the construction shown in Fig. 6, it follows that the vector distance between a pair of atoms, $\mathbf{r}^{ij}_{lmn}$, has radial and tangential displacement components with magnitudes given by:

$$\left|\bar{\delta}^{ij}_{lmn}\right|_{\|} = \frac{\bar{\delta}^{ij}_{lmn} \cdot \mathbf{R}_{lmn}}{\left|\mathbf{R}_{lmn}\right|} \qquad \text{(Eq 15a)}$$

and

$$\left|\bar{\delta}^{ij}_{lmn}\right|_{\perp} = \sqrt{\left|\bar{\delta}^{ij}_{lmn}\right|^2 - \left|\bar{\delta}^{ij}_{lmn}\right|^2_{\|}} \qquad \text{(Eq 15b)}$$

The radial (||) and tangential (⊥) components of the displacements recovered from diffuse scattering measurements on single crystals are shown in Fig. 6.

Because the $Fe_{46.5}Ni_{53.5}$ alloy is cubic (face centered), the $\Delta\mathbf{Y}$ and $\Delta\mathbf{Z}$ displacements are derived from the $\Delta\mathbf{X}$s given in Table 2 by permutation of the indices. (Henceforth, the <> will be dropped from the displacements for simplicity.) For example, $\Delta\mathbf{X}_{321}$ has the identical value as $\Delta\mathbf{Y}_{231}$ and as $\Delta\mathbf{Z}_{123}$, and $\Delta\mathbf{X}_{321} = \Delta\mathbf{X}_{312} = \Delta\mathbf{Y}_{231} = \Delta\mathbf{Y}_{132} = \Delta\mathbf{Z}_{123} = \Delta\mathbf{Z}_{213}$. In addition, $\Delta\mathbf{X}_{321} = -\Delta\bar{\mathbf{X}}_{321}$ and similarly for the other combinations as illustrated in Fig. 7 (Ref 25). The nearest atom pairs that could exhibit nonradial components are those in the third neighboring shell, lmn = 211.

If the displacements between atom pairs is, on the average, along their interatomic vector, then $\Delta\mathbf{X}_{211} = 2\Delta\mathbf{X}_{121}$. For the Fe-Fe pair, displacements given in Table 2, $\Delta\mathbf{X}_{211}$ = 0.0005(2) Å and $2\Delta\mathbf{X}_{121}$ = 0.0028(8) Å, thus the (211) Fe-Fe pair displacements have a significant tangential component. From Eq 15(a) and (b), the magnitude of the displacement between (211) Fe-Fe pairs along the radial direction $\left|\bar{\delta}^{\text{Fe-Fe}}_{211}\right|_{||}$ is 0.0016(7) Å and $\left|\bar{\delta}^{\text{Fe-Fe}}_{211}\right|_{\perp}$ tangential is 0.0013(7) Å. Thus the (211) Fe-Fe neighbors have a similar radial and tangential component to their displacements. For the (310) Fe-Fe pair displacements, $\Delta\mathbf{X}_{310} \approx 3\ \Delta\mathbf{X}_{130}$ within the total estimated error, and on the average (310) displacements are predominantly radial. These measured displacements provide new information not obtained in other ways about the local atomic arrangements in crystalline solid solutions.

Only a few crystalline binary alloys have had their individual pair displacements measured with this 3λ technique. They include $Fe_{22.5}Ni_{77.5}$ (Ref 1, 4), $Fe_{46.5}Ni_{53.5}$ (Ref 4), $Cr_{47}Fe_{53}$ (Ref 2), and $Cr_{20}Ni_{80}$ (Ref 3). These results are summarized in Fig. 8, where the $\Delta\mathbf{X}$ static displacements are plotted as a function of the radial distance $\frac{1}{2}\sqrt{l^2 + m^2 + n^2}$. When there is more than one value for $\Delta\mathbf{X}$, the plots show the various values. Most striking is the observation that for the three ordering alloys, the near-neighbor Fe-Ni and Cr-Ni bond distances are the smallest of the three possible pairs (Fig. 8a to c). However, for the clustering $Cr_{47}Fe_{53}$ alloy, the Cr-Cr nn bond distances are closest and the Cr-Fe farthest apart. More details including the short-

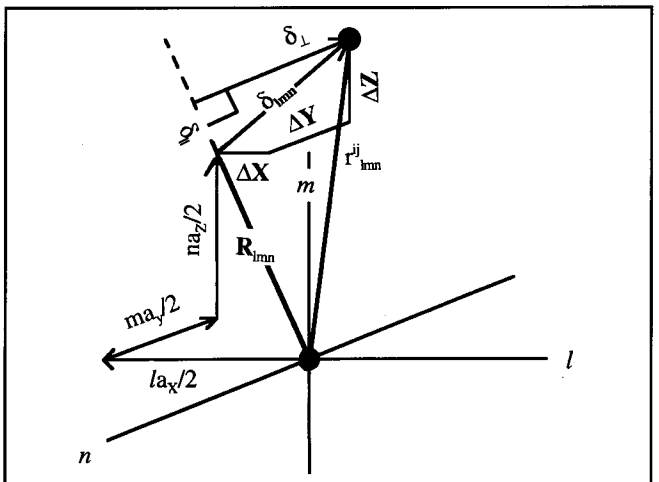

Fig. 6 Construction of the vectors recovered from diffuse scattering measurements on single crystals. $\mathbf{R}_{lmn}$ is obtained from the lattice parameter a, and the average components of the displacement $\bar{\delta}^{ij}_{lmn}$ are recovered from measurements of the diffuse scattering.

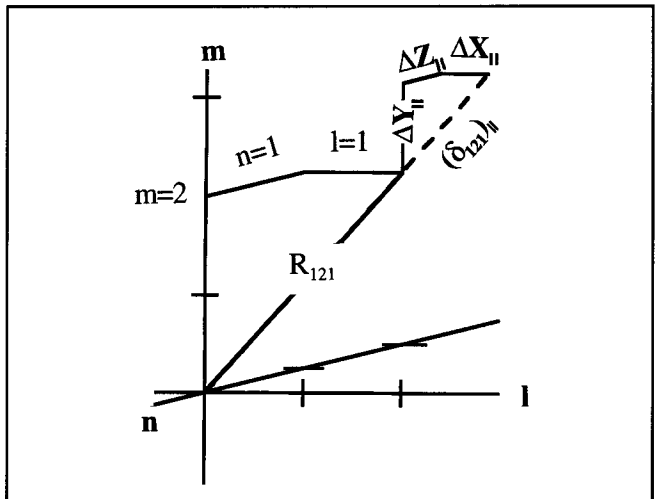

Fig. 7 Radial displacements (parallel to the interatomic vector $\mathbf{R}_{lmn}$) between the atom pairs require that the relative magnitudes of the displacement components be in the same proportion as the average lattice vector; $\Delta\mathbf{X}$:$\Delta\mathbf{Y}$:$\Delta\mathbf{Z}$ = l:m:n. As shown for lmn = 211, a radial displacement requires $|\Delta\mathbf{X}| = 2|\Delta\mathbf{Y}|$ and $|\Delta\mathbf{X}| = 2|\Delta\mathbf{Z}|$. For lmn = 121, $|\Delta\mathbf{X}| = |\Delta\mathbf{Y}|/2$ and $|\Delta\mathbf{X}| = |\Delta\mathbf{Z}|$. For a cubic lattice l, m, and n can be interchanged, and similarly, $\Delta\mathbf{X}$, $\Delta\mathbf{Y}$, and $\Delta\mathbf{Z}$. Thus there is only one value $\Delta\mathbf{X}$ for lmn multiplicities <24, i.e., 110, 200, 222, etc., two values for $\Delta\mathbf{X}$ when lmn has multiplicities equal to 24 ($l \neq m$ and $l = m,n$), and three values for $\Delta\mathbf{X}$ with multiplicities equal to 48.

range order parameters α and numerical values of the displacements for each shell are given in the original papers. These pair displacement observations provide a more rigid test of theoretical predictions than variations of the average lattice parameter with concentration (Ref 26, 27).

Chakraborty (Ref 28) has proposed a compressible Ising model that can qualitatively reproduce the observed shortened nn bond distance for Fe-Ni pairs and the expanded Cr-Fe pairs. In this model there is a "size effect" term, which reflects the different size of the atoms, and an "Ising" term, which is sensitive to the distance-dependent Ising interaction. For systems such as the Fe/Ni/Cr binary alloys where the "size" of the atoms is similar, the unlike pair displacements do not necessarily lie between the observed like-atom displacements. Small cluster calculations appear to be another useful tool for studying the mechanisms behind the observed displacements. The relationship between local strains and overall lattice spacing is of great interest. Recent calculations on small 12 to 18 atom clusters reproduce some of the observed displacement trends in Fe-Ni alloys, but the results are complicated by large surface and concentration effects (Ref 29). An imbedded cluster calculation could eliminate surface effects and lead to a more complete understanding of the forces driving the observed static displacements. For a recent review of the information recovered from diffuse scattering measurements and its role in testing theoretical concepts, see Ref 30.

5. Conclusions

The displacements of the atoms from the sites of the average lattice can be recovered from diffuse x-ray scattering measurements on single crystals. These measured displacements include information on the dynamic and static displacements and on the chemically sensitive local bond lengths. The expectations of the vector displacements are recovered, including the radial, and, unique to these measurements, the tangential displacement components. Analysis of the statistical and systematic errors shows that the value of these static displacements is statistically significant. Such measurements provide new information on the real structure of crystalline solid solutions for comparison with theoretical modeling.

Acknowledgment

The authors wish to express their gratitude to Eliot Specht and Jin-Seok Chung for their comments on this manuscript. X. Jiang is supported through Sandia National Laboratory by a New Initiative from the U.S. Department of Energy, Office of Basic Energy Sciences, Division of Materials Sciences, under Contract No. DE-AC04-94AL85000. This research was performed in part at the ORNL/MRS beamline X-14 at the National Synchrotron Light Source, Brookhaven National Laboratory, sponsored by the Division of Materials Sciences and Division of Chemical Sciences, U.S. Department of

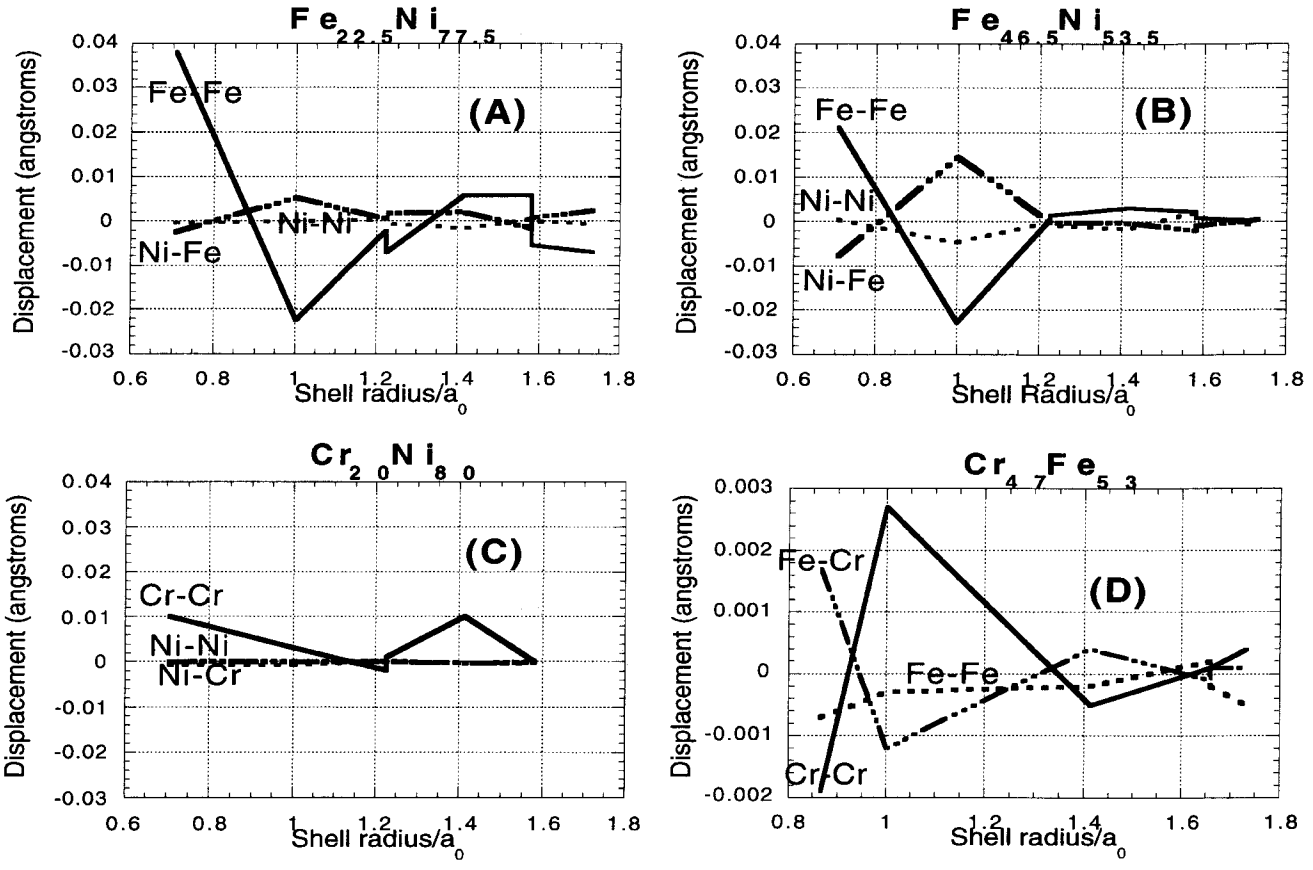

Fig. 8 Displacement from the average lattice sites for chemically specific pairs. Shell radius divided by the lattice parameter a_0 becomes 1 for second neighbors (separated by the cube edge). Source: Ref 2 to 4.

Energy, under Contract No. DE-AC05-96OR22464 with Lockheed Martin Energy Research Corporation.

Cited References

1. G.E. Ice, C.J. Sparks, A. Habenschuss, and L.B. Shaffer, *Phys. Rev. Lett., 68,* 863 (1992).
2. L. Reinhard, J.L. Robertson, S.C. Moss, G.E. Ice, P. Zschack, and C.J. Sparks, *Phys. Rev. B, 45,* 2662 (1992).
3. B. Schönfeld, G.E. Ice, C.J. Sparks, H.G. Haubold, W. Schweika, and L.B. Shaffer, *Phys. Status Solidi (b), 183,* 79 (1994).
4. X. Jiang, G.E. Ice, C.J. Sparks, L. Robertson, and P. Zschack, *Phys. Rev. B, 57,* 3211 (1996).
5. L. Vegard, *Z. Kristallogr., 67,* 239 (1928).
6. C.J. Sparks, G.E. Ice, X. Jiang, and P. Zschack, *Mater. Res. Soc. Symp. Proc., 375,* 213 (1995).
7. G.E. Ice, C.J. Sparks, J.L. Robertson, J.E. Epperson, and X. Jiang, *Mater. Res. Soc. Symp. Proc., 437,* 181 (1996).
8. F. Laves, *Crystal Structure and Atomic Size in Theory of Alloy Phases,* American Society for Metals, Cleveland, OH, 124 (1956).
9. R.L. Fleischer, *Acta Metall., 11,* 203 (1963).
10. W. Hume-Rothery, *The Structure of Metals and Alloys,* Institute of Metals, London (1963).
11. A. Zunger, *Statics and Dynamics of Alloy Phase Transitions,* Vol. B319, *NATO ASI Series B,* P.E.A. Turchi and A. Gonis, Ed., Kluwer, Dordrecht, 361 (1994).
12. U. Scheuer and B. Lengeelr, *Phys. Rev. B, 44,* 9883 (1991).
13. G. Renaud, N. Motta, F. Lançon, and M. Belakhovsy, *Phys. Rev. B, 38,* 5944 (1988).
14. B.E. Warren, B.L. Averback, and B.W. Roberts, *J. Appl. Phys., 22,* 1493 (1951).
15. B. Borie and C.J. Sparks, *Acta Crystallogr. A, 17,* 198 (1971).
16. G.E. Ice, C.J. Sparks, and L. Shaffer, *Resonant Anomalous X-Ray Scattering: Theory and Experiment,* G. Materlik, C.J. Sparks, and K. Fischer, Ed., North-Holland, Amsterdam, 265 (1994).
17. B.E. Warren, *X-Ray Diffraction,* Dover, New York (1969).
18. C.B. Walker and D.T. Keating, *Acta Crystallogr., 14,* 1170 (1961).
19. F.H. Herbstein, B.S. Borie, Jr., and B.L. Averbach, *Acta Crystallogr., 9,* 466 (1956).
20. C.J. Sparks, G.E. Ice, L.B. Shaffer, and J.L. Robertson, *Metallic Alloys: Experimental and Theoretical Perspectives,* Vol. 256, *NATO Series,* J.S. Faulkner and R.G. Jordan, Ed., Kluwer Academic Publishers, Dordrecht, 73 (1994).
21. X. Jiang, G.E. Ice, C.J. Sparks, and P. Zschack, "Applications of Synchrotron Radiation Techniques to Materials Science," *Mater. Res. Soc. Symp. Proc., 375,* 267 (1995).
22. X. Jiang, J.L. Robertson, G.E. Ice, and C.J. Sparks, to be published.
23. C.J. Sparks, *Phys. Rev. Lett., 33,* 262 (1974).
24. J.L. Robertson, G.E. Ice, C.J. Sparks, X. Jiang, P. Zschack, F. Bley, S. Lefebvre, and M. Bessiere, to be published.
25. C.J. Sparks and B. Borie, *Local Atomic Arrangements Studied by X-Ray Diffraction,* J.B. Cohn and J.E. Hilliard, Ed., Vol. 36, Metallurgical Society Conferences, Gordon and Breach, New York, 5 (1965).
26. S. Froyen and C. Herring, *J. Appl. Phys., 52,* 7165 (1981).
27. N. Mousseau and M.F. Thorpe, *Phys. Rev. B, 45,* 2015 (1992).
28. B. Chakraborty, *Europhys. Lett., 30,* 531 (1995).
29. G.E. Ice, G.S. Painter, L. Shaffer, and C.J. Sparks, *Nanostructured Mater., 7*(1-2), 147 (1996).
30. W. Schweika, *Statics and Dynamics of Alloy Phase Transformations,* P.E.A. Turchi and A. Gonis, Ed., Plenum Press, New York, 103 (1994).